Chapter 2

Electrochemical Detection of Azidothymidine on Modified Sensor Probes based on Chitosan Stabilised Silver Nanoparticles Hybrid Materials

2.1 Introduction

Acquired immunodeficiency syndrome (AIDS) is an immunosuppressive disease, which is caused by HIV-1 (Human immunodeficiency virus-1). 3'-azido-3'-deoxythymidine (Zidovudine or Retrovir or Azidothymidine or AZT), a nucleoside reverse transcriptase inhibitor (NRTI), is considered to be safe and effective for curing HIV. It is officially approved and commercialised as Retrovir in 1987. AZT is still extensively used as antiretroviral (ARV) drug for the treatment of persons infected with HIV-1 [Hirsch *et al.*, 1993; Barone *et al.*, 1991; Hoetelmans *et al.*, 1996; Font *et al.*, 1999; Clercq *et al.*, 1994; Warnke *et al.*, 2007]. Due to its undesirable side effects and short therapeutic interval, the determination of AZT in human serum is the most important for patient's health. The toxic side effects are generally exhibited when the patient's serum concentration is above 10 µM [Clercq *et al.*, 2004; Chiu *et al.*, 1995]. Various methods like chromatography [Quevedo *et al.*, 2006], radioimmunoassay (RIA) [Granich *et al.*, 1989], fluorescence spectroscopy, fluorescence polarisation immunoassay (FPIA) [Raviolo *et al.*, 2008] and electrochemical technique [Leandro *et al.*, 2010; Peckova *et al.*, 2009] have been proposed for the determination of AZT. Among these methods, electrochemical technique exhibits great attention due to fast response, high sensitivity and low cost as well as easy development of user-friendly appliances and disposable screen printed electrode. In general, the azido group (present in AZT) is considered as an antiviral agent as well as the basis of electrochemical analysis during electrochemical

reduction clinically [Trnkova *et al.*, 2004; Mattson *et al.*, 2009; Sosnik *et al.*, 2009; Vacek *et al.*, 2011; Peng *et al.*, 2011].

Metal nanoparticles have exhibited great attention due to their significant contribution in wide areas of science and technology including catalysis, photonics, chemical sensor and biosensor [Sau *et al.*, 2010; Nigra *et al.*, 2013; Huang *et al.*, 2013; Gupta *et al.*, 2014]. Particularly, noble metal nanoparticle like Ag, Au, Pt, Pd, *etc.* exhibits great attention due to their biostability, high spectral properties and easy functionalization. Among these metal nanoparticles (NPs), most of the electrochemical sensing is based on Au NPs and Ag NPs [Gupta *et al.*, 2014; Chang *et al.*, 2011]. However, the aggregation of nanoparticles restricts their usage as an active material for sensors and so far. Therefore, stabilization of these nanomaterials by incorporation of foreign material like polymer, or macromolecules is one of the most common choices to reduce its aggregation. In addition, it is also useful to provide a suitable matrix for modification of sensing probes. For instance, the functionalization of Ag NPs with appropriate molecules like citric acid and phenothiazine, and polymeric matrix like protein, poly [4-(thiophen-3yl)-aniline is of great interest particularly in sensor and catalysis application [Gupta *et al.*, 2014; Bastus *et al.*, 2014; Bayram *et al.*, 2015; Negm, *et al.*, 2015; Choudhary *et al.*, 2014]. Chitosan (Ch) is an environmentally friendly biopolymer and considered as an excellent stabilizing agent for nanoparticles due to its biocompatibility, low toxicity and high adsorption properties [Zeng *et al.*, 2014; Wei *et al.*, 2009]. Recently, we have demonstrated excellent film formation of metal stabilised Ch for sensing applications [Kashish, *et al.*, 2015; Srivastava *et al.*, 2014]. Literature survey exemplifies that most of the work is devoted for AZT detection based on HMDE (Hanging mercury drop electrode) [Kobayashi *et al.*, 1996; Leandro *et al.*, 2010; Peckova *et al.*, 2009]. However, few works have been reported based on conducting

polymer composite modified graphite paste electrode and Ag-MWCNT composite nanofilm modified glassy carbon electrode [Mohan *et al.*, 2010; Rafati *et al.*, 2014]. In spite of their advantages, these techniques require complicated processing for AZT detection. At the same time, reuse of commercial electrodes may not be suitable for on-site measurement because its operation is time consuming and requires highly trained users. Therefore, disposable screen printed graphite electrode (SPGE) is one of the best choices to overcome these issues. This is due to its cost effectiveness and easiness in electrode assembly (in a single matt), which make it well suited for mass production of portable devices.

To the best of our knowledge, the utilisation of Ch stabilised Ag NPs modified SPGE portable probe towards electrochemical sensing of AZT is not yet been reported. In this work, we are reporting the development of low cost portable sensors based on Ch@Ag NPs/SPGE probes. Also, the performance of Ch@Ag NPs/SPGE probes have been compared with Ch@Ag NPs modified commercial GCE in buffer and real biological samples.

2.2 Experimental Details

2.2.1 Materials

AZT is purchased from Sigma Aldrich, U.S.A. Glacial acetic acid; $AgNO_3$ and Milli Q water are purchased from Merck, India. $NaBH_4$ is obtained from SRL Pvt. Ltd. Chitosan (lower molecular weight Chitosan (poly-(D-glucosamine) =<5400g/mol, degree of deacetylation = 84.5%) is brought from Sigma Aldrich. All used reagents are of analytical grade. Phosphate Buffer solution (PBS) of 0.1 M is prepared using NaH_2PO_4 and Na_2HPO_4 (SRL Pvt. Ltd.). All solutions are prepared using double distilled water,

and deoxygenated by purging high purity (99.99%) nitrogen gas for 10 minutes prior to each experiment. All experiments are performed at room temperature (25 ºC). Screen printed graphite electrodes (SPGE; WE diameter =2.5 mm, CE and RE width =1.25 mm) are purchased from PalmSens BV, The Netherlands.

2.2.2 Synthesis of Ch@Ag NPs material

In a typical synthesis of Ch@Ag NPs, 10 mL of 2.5 % stock solution of Chitosan is prepared in 1.0 % acetic acid solution. After that, 2 mL aqueous solution of $AgNO_3$ (17 mM) is mixed with 5 mL Chitosan stock solution. Thus, the prepared solution is kept on stirring for 4 h. This mixture is then reduced by 100 µL $NaBH_4$ (0.04 M). The resulting solution is centrifuged and washed several times with Milli-Q water, to remove unreacted $AgNO_3$, NO_3^- and other dissolved impurities. Finally, as-synthesized Ch@ AgNPs is preserved in dark in refrigerator at 4 ºC and used directly for its next experimentations [Chen *et al.*, 2013].

2.2.3 Instrumentation

As-synthesized Ch@Ag NPs is characterized for its structural, morphological and electrochemical properties by means of following instrumental techniques. UV -Vis. spectral changes are observed with Lambda-25 spectrophotometer, Perkin Elmer, Germany. Zeta potential measurement is performed on Nanoparticle Analyzer SZ-100, Japan. FT-IR spectra are obtained using Nicolet 6700 FTIR spectrophotometer, USA. SEM images are taken with the help of FESEM, Curl Zeiss Supra 40, Germany. TEM measurement is executed using HRTEM Tecnai G2, 20 FEI Corporation, the Netherlands operating at 200kV. Voltammetric analysis are performed using CH-instrument (electrochemical workstation, model CH17041C) Inc. USA as well as

experiments based on screen printed graphite electrode are executed with PS Trace PalmSens3 (Handheld Potentiostat/ Galvanostat), The Netherlands. Herein former instrument represents reduction with positive current direction while latter instrument represents reduction in negative current direction due to its own default sign convention. Conventional three electrode cell assembly employing GCE or SPGE as working electrode (WE), Pt as counter electrode (CE) and Ag/AgCl as reference electrode (RE) is utilised to study the electrochemical and sensing behaviour. A calibration plot for each sensing measurement is drawn between change in reduction peak current *vs.* AZT concentration in order to determine the LOD and sensitivity of as-fabricated sensing probe. The change in reduction current is calculated by the subtraction of bare current response (without addition of AZT) from actual current response.

2.2.4 Electrode modification

Prior to the electrode modification, cleaning of commercial GCE (diameter=3.0 mm) and Pt electrode (diameter=3.0 mm) are performed thoroughly using 0.05 µm alumina slurry followed by ultrasonication in ethanol and distilled water sequentially for 10 minutes. Afterwards, 5.0 µL of 2.0 mg Ch@Ag NPs dispersion (in 500 µL distilled water) is drop cast over the commercial GCE (disc diameter = 3 mm) and dried in a vacuum desiccator. Similar to above procedure, 5.0 µL of 2.0 mg Ch@Ag NPs dispersion (in 500 µL distilled water) is used for the modification of working electrode of SPGE.

2.3 Results and discussion

The basis of Ch capping on Ag NPs in Ch@Ag NPs and its usage as conducting matrix for AZT sensing is shown schematically in Figure 2.1. Various possible interactions

between all components are also explained in Figure 2.1. On addition of a calculated amount of Chitosan to acetic acid, protonation of an amino group (of Ch) takes place and hence it acts as cationic polymer. Probably a coordination interaction takes place between Ag (I) and electron rich moiety of cationic Ch polymer on addition of aq. $AgNO_3$ in Ch polymer solution [Chen *et al.*, 2013]. Ch@Ag NPs formed after addition of aq. $NaBH_4$ in above coordinated solution mixture. Similarly, a synergic interaction (between Ag NPs and –OH/C=O: of AZT) was the basis of adsorption of AZT over Ch@Ag NPs matrix. Herein, AgNPs synergistically interact with electron rich functionalities present in Ch matrix as well as AZT (as shown in inset of Figure 2.1). In view of above, we tried to exemplify the sensing of AZT over Ch@Ag NPs modified commercial GCE and SPGE experimentally as explained one by one.

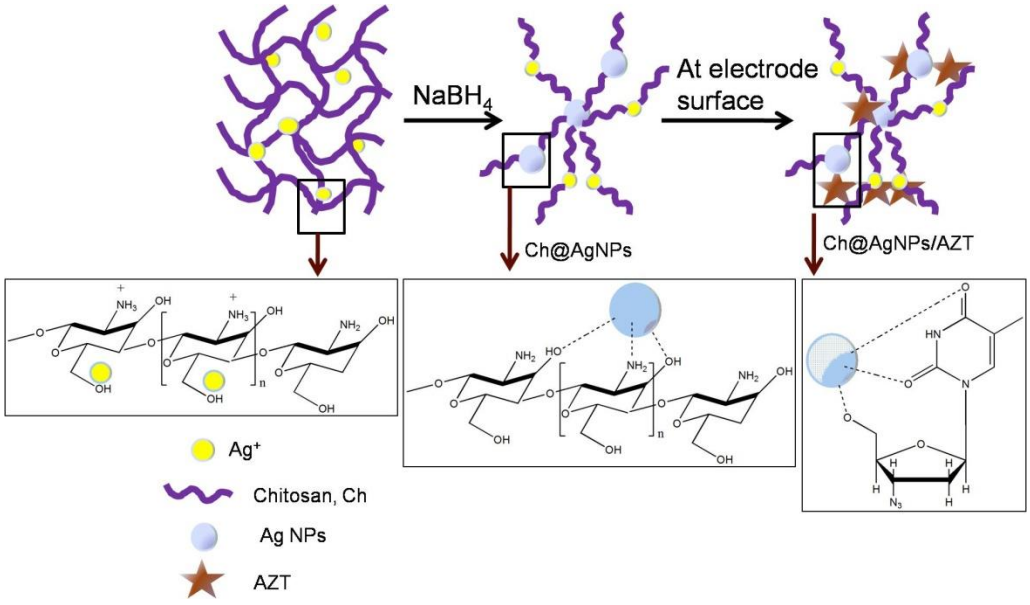

Figure 2.1 Schematic representations for various interactions between components used for Ch@Ag NPs formation and AZT sensing.

2.3.1 Characterization of Ch@Ag NPs

2.3.1.1 UV-vis. Absorption studies

The reduced form of Ag and its interaction with Ch matrix is analyzed by UV- visible absorption spectrum under baseline correction using water to avoid misconceptions related to peak of water (as shown in Figure 2.2). Ch is expected to be a cationic polymer due to protonation of amino group present in the molecule (as it is only soluble in acid) [Huang *et al.*, 2004]. Therefore, a broad hump near 210 nm is observed due to electronic excitation for electron pair on oxygen (-OH group) of Ch (as shown in inset of Figure 2.2) in UV-visible spectrum. However, as-prepared Ch@Ag NPs shows a broad absorption band at 437 nm for characteristic surface Plasmon resonance of reduced Ag NPs and a new absorption peak at 212 nm indicates interaction of oxygen of Ch with reduced Ag NPs [Chen *et al.*, 2013]. The Plasmon resonance peak for Ag NPs is size dependent and observed a red shift with an increase of particle size [Novo et al, 2009].

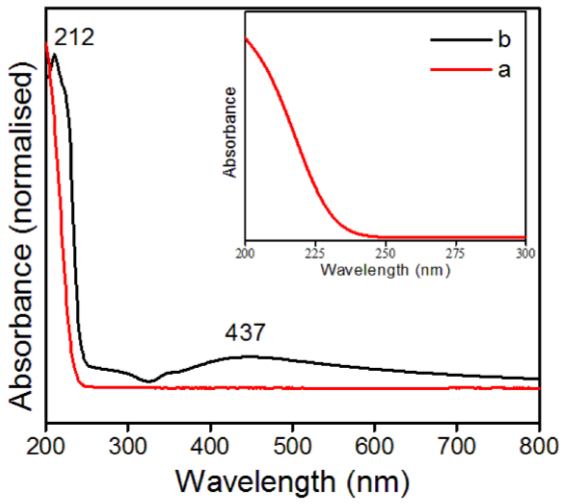

Figure 2.2 UV-visible spectra of (a) Ch and (b) Ch@Ag NPs in water. Inset shows zoomed view of Ch from 200 nm to 300 nm.

The dispersion stability of as-prepared Ch@Ag NPs in water is determined spectroscopically by zeta potential (ζ) measurement that indicates the changes occurred

on the surface of Ch@Ag NPs with respect to time. For an ideal dispersion, the ζ value more than +30 and -30 is considered to be stable [Melendrez *et al.*, 2010]. The ζ value of our as-prepared Ch@Ag NPs is +38.2 mV (Figure 2.3), which indicates its high stability in water over a long period of time.

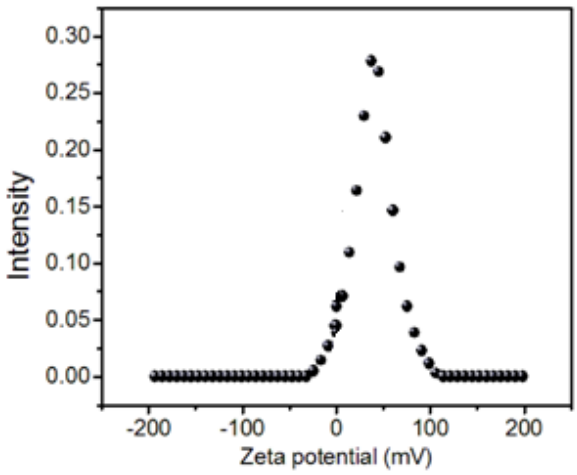

Figure 2.3 Surface zeta potential graph of Ch@Ag NPs.

2.3.1.2 FT-IR analysis

The electrostatic interaction between Ag NPs with the Ch matrix is again investigated by FT-IR as shown in Figure 2.4. In general, Ch exhibits major absorption bands at 891 cm^{-1} and 1152 cm^{-1} that can be attributed to the glycosidic bonding [Yang *et al.*, 2007]. The characteristics bands at 3433 cm^{-1} (stretching vibration of –OH and –NH groups), 2879 cm^{-1} (symmetric stretching vibration of $–CH_3$ group in amide linkages), 1647 cm^{-1} (stretching vibration of C=O groups), 1420 cm^{-1} (vibration of the primary alcoholic group) and 1574 cm^{-1} (bending vibration of N-H group) are assigned from the literature as shown in Figure 2.4a [Wang *et al.*, 2010; Ghavale *et al.*, 2009; Rao *et al.*, 2010]. However, a decrease in these vibration peaks is observed in case of Ch@Ag NPs. For example the peak at 3433 cm^{-1} shifted to 3420 cm^{-1}, the peak at 1653 cm^{-1} shifted to

1636 cm^{-1} and the peak at 1420 cm^{-1} shifted to 1387cm^{-1} (as shown in Figure 2.4b). These shifts of wave number of stretching and bending vibration of N-H, O-H and symmetric stretching vibration of C=O groups suggest that there is an interaction between Ag NPs and Ch matrix due to transfer of the electron density from C and N atoms to the Ag atoms.

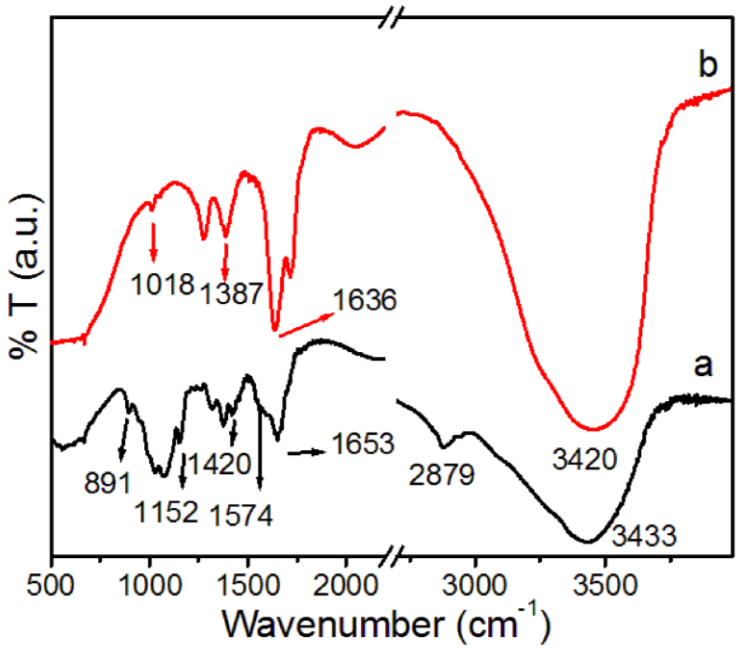

Figure 2.4 FT-IR spectrum of (a) Ch and (b) Ch@Ag NPs.

2.3.1.3 EDAX analysis

The reduction of Ag is confirmed by EDAX as shown in Figure 2.5. The EDAX spectrum exhibits that Ch@Ag NPs contains C, N, O and Ag elements with 23.95, 38.44, 3.50 and 34.11 wt. % respectively recorded for an enclosed square area. From this spectrum, it is exemplified that presence of a strong signal near 3 keV is due to surface Plasmon resonance of metallic Ag [Kalimuthu *et al.*, 2008].

EDAX mapping of Ch@Ag NPs confirms the homogeneous distribution of all elements present like Carbon, Nitrogen, Oxygen and Silver.

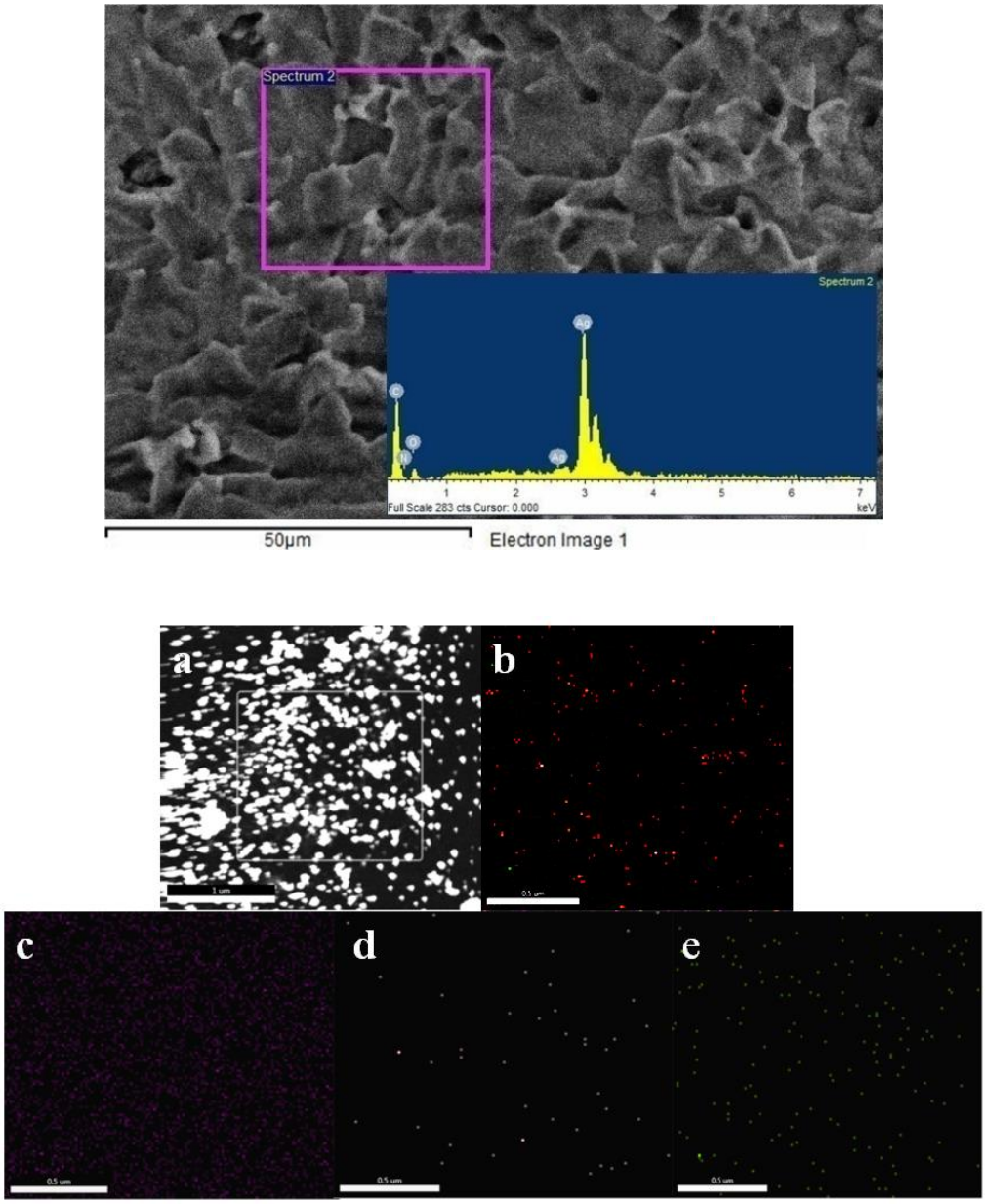

Figure 2.5 EDAX spectrum and mapping of Ch@Ag NPs [a) STEM image area selected for mapping, b) EDAX mapping of Ch@Ag NPs, Individual mapping of elements c) Carbon d) Nitrogen e) Oxygen].

2.3.2 Morphological analysis

The surface texture of Ch and Ch@Ag NPs is analyzed by FESEM images as shown in Figure 2.6. From this Figure it is evident that Ch matrix is forming globular, uniform and dense film (as shown in Figure 2.6a) which is holding Ag NPs (as shown in Figure 2.6b).

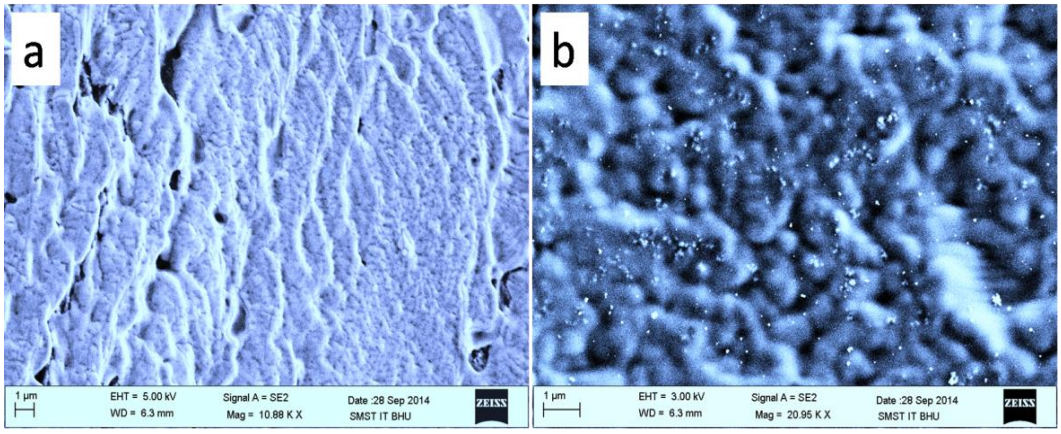

Figure 2.6 SEM of (a) Ch and (b) Ch@Ag NPs.

These Ag NPs in Ch@Ag NPs exist in its reduced state which is observed by TEM after completion of the reaction (as shown in Figure 2.7a). Herein we observed similar texture of particles as seen earlier by FESEM. These particles exhibit various diffraction patterns corresponding to reduced Ag as observed by selected area electron diffraction (SAED) pattern (as shown in Figure 2.7b). From this pattern, it can be concluded that Ag NPs are crystalline in nature showing Scherrer rings corresponding to (111), (200) and (220) planes of *fcc* lattice. The average particle size distribution of as-prepared Ch@Ag NPs lies in the nanometric range from 20 nm to 30 nm calculated from Figure 2.6a using standard Image J software (shown in Figure 2.7c).

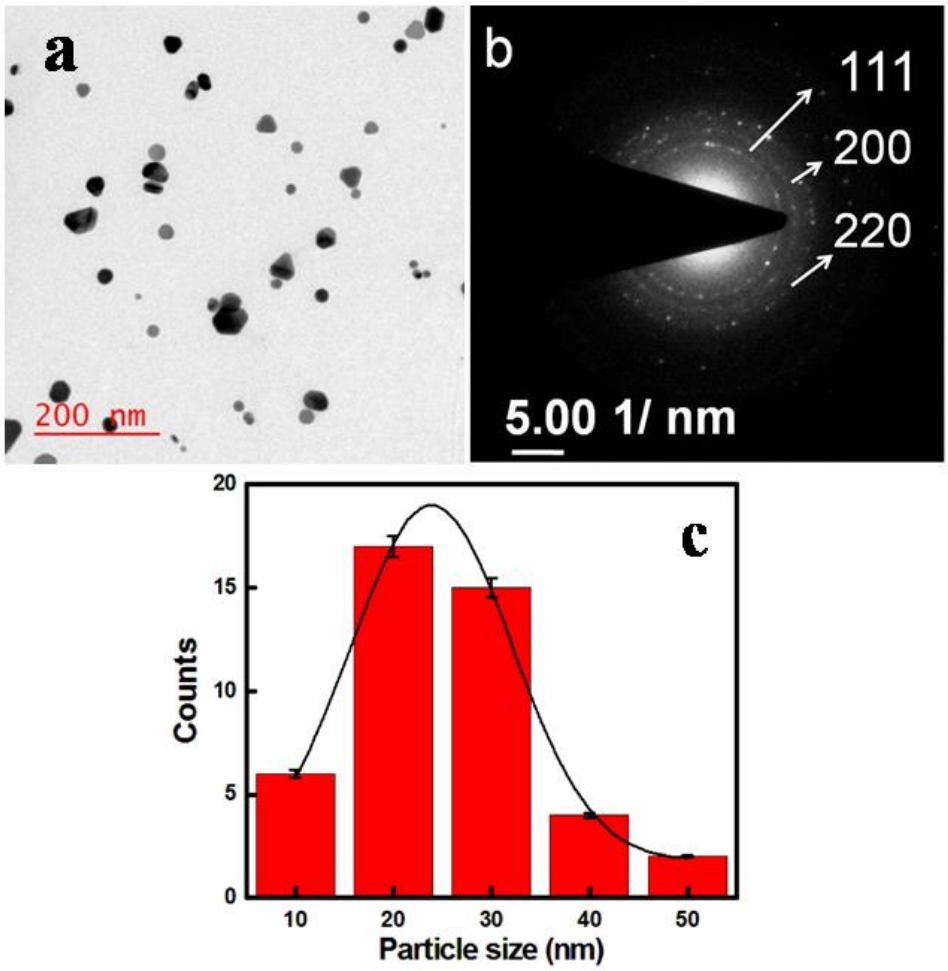

Figure 2.7 (a) TEM image, (b) SAED pattern and (c) particle size distribution of Ch@Ag NPs.

2.3.3 Electrochemical analysis of AZT

In general interpretation, the electrochemical reduction behaviour of AZT is observed due to the presence of azido group. The azide group exhibits electro-reduction that depends on pH of the medium used for analysis. When the medium is alkaline, the reduction is proposed *via* $2H^+$ and four electron transfer processes [Vacek *et al.*, 2004]. In above view, commercial GCE, commercial Ag electrode and as-modified Ch@Ag NPs/GCE are checked carefully first for its electrochemical activity towards AZT

reduction and then, applied for various concentration of AZT determination. The stepwise experimentations are described as follows:

Prior to AZT detection, Ch@Ag NPs/GCE is checked for its redox behaviour and compared with commercial GCE by performing CV in PBS (pH = 7.6) as shown in Figure 2.8. It exhibits Ag oxidation peak at +0.34 V and its corresponding reduction peak at -0.026 V. However, such type of redox behaviour is not observed in case of bare commercial GCE (Figure 2.8a and Figure 2.8b). After that, Ch@Ag NPs modified electrode is compared with macro electrodes, i.e., commercial Ag and GCE at a fixed concentration for the AZT reduction as shown in Figure 2.9. In this experiment, 5.0 µL of 2.0 mg Ch@Ag NPs dispersion (in 500 µL distilled water) is loaded over commercial GCE and compared with bare GCE and commercial Ag electrode for its electrochemical response (CV) towards AZT reduction. On comparing the reduction peaks of AZT, we observed that Ch@Ag NPs/GCE successfully gives reduction peak for AZT at -0.60 V (Figure 2.9b and Figure 2.9c). However, this peak shifts towards positive side (-0.45 V) in case of commercial Ag electrode. The shift in peak potential of modified electrode is probably due to insulating nature of Chitosan film. Herein more energy input is required due to insulation or high impedance of the electrode in case of Ch modification.

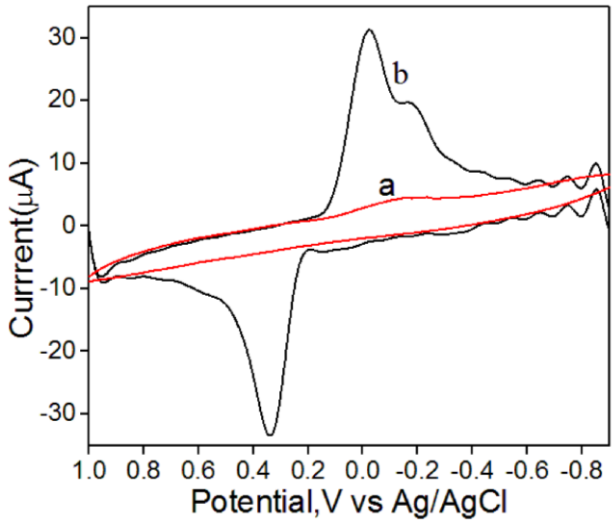

Figure 2.8 CV of (a) Commercial GCE and (b) Ch@Ag NPs/GCE in 0.1 M PBS (pH 7.6).

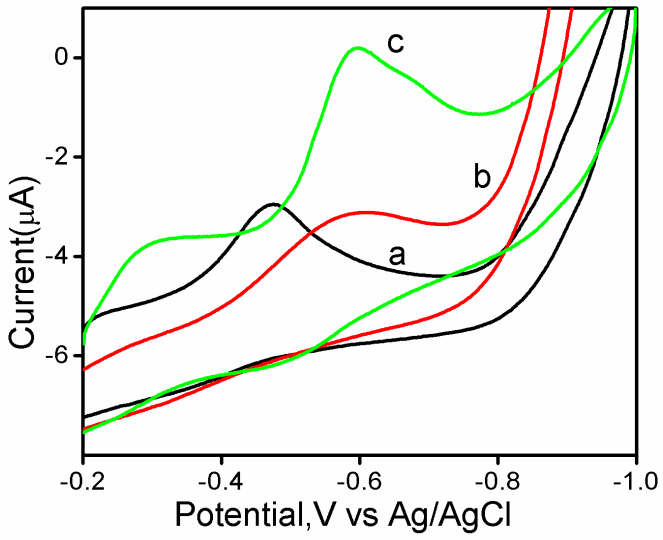

Figure 2.9 CV of (a) bare commercial Ag electrode, (b) bare commercial GCE and (c) Ch@Ag NPs/GCE in presence of AZT in 0.1 M PBS (pH = 7.6).

Further, the catalytic effect of the modified electrode is observed in terms of peak current when difference in reduction current (Δi) is calculated for two different concentrations of AZT solution (295 µM and 439 µM) by performing CV at fixed scan

rate for both the electrodes, i.e., modified and commercial Ag electrodes. We observed Δi=1.44 µA for commercial Ag and Δi=2.24 µA for Ch@Ag NPs/GCE, indicating catalytic effect of Ch@Ag NPs/GCE. This catalytic effect is due to coordination of AZT with modified electrode and large energetic surface of Ag NPs (shown in Figure 2.10). The catalytic effect of Ch@Ag NPs/GCE is compared with commercial Ag electrode towards AZT reduction as shown in Figure 2.10.

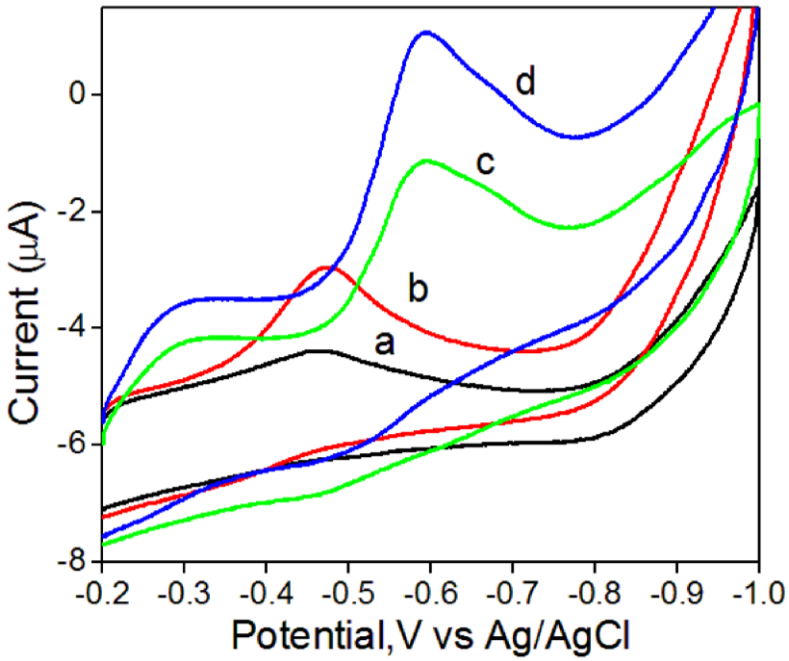

Figure 2.10 CV of 295 µM and 439 µM AZT over commercial Ag electrode (a & b) and Ch@Ag NPs/GCE (c & d) at scan rate 50 mV/s.

After that Ch@Ag NPs/GCE is again checked for its time dependent reliability during the course of AZT reduction. The reliability of as-modified Ch@Ag NPs/GCE electrode is checked with respect to time interval at a scan rate of 50 mV/s as shown in Figure 2.11. In this technique, CV of a fixed concentration of AZT reduction is performed at constant scan rate for several cycles (as shown in Figure 2.11-a) and then again scanned after a time 10, 15, 20 minute (as shown in Figure 2.11-b to Figure 2.11-d). We observed that our modified electrode exhibits constant peak voltage and current initially

for more than 10 cycles as shown by an overlapped thick green colour curve. However, reduction current goes on decreasing gradually at constant reduction potential whenever scanning is again started after 10, 15 and 20 minutes. It means that the active sites of modified electrode are blocking/ poisoning by AZT.

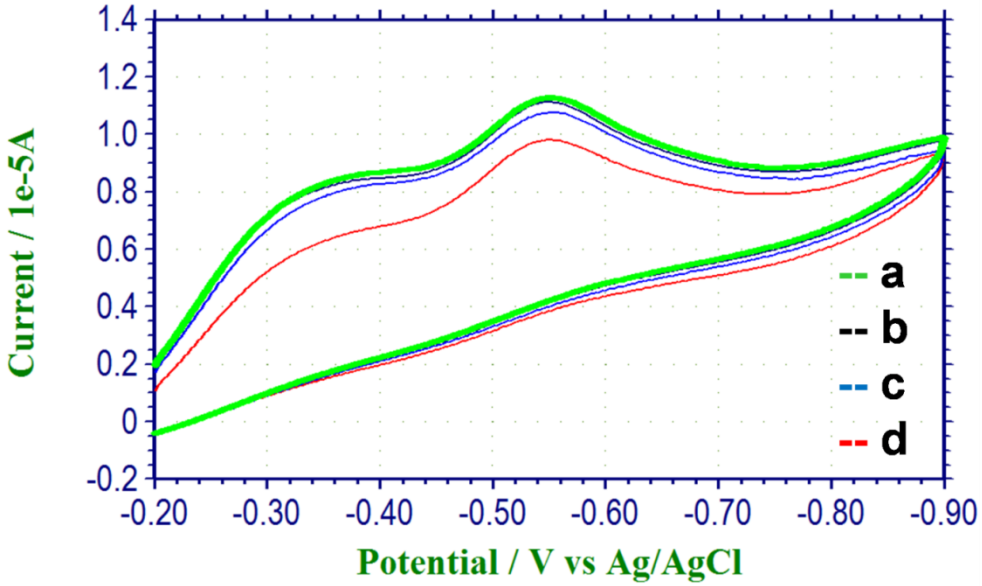

Figure 2.11 CV of 100 µM AZT over Ch@Ag NPs/GCE at a scan rate 50 mV/s.

2.3.3.1 Effect of scan rate

The electron transfer characteristics of Ch@Ag NPs/GCE is checked and compared with commercial GCE and commercial Ag electrodes at different scan rate ranging from 10 to 500 mV/s (as shown in Figure 2.12 a-c). From these voltammograms, it is evident that the reduction peak current of AZT increases in a linear fashion with the increasing value of square root of scan rate in all cases but with different slopes (as shown in Figure 2.12 d). It means that the electrochemical reduction of AZT on Ch@Ag NPs/GCE is diffusion controlled process and depicts fast electron transfer rate as compared to bare commercial GCE and commercial Ag electrode. The fast electron transfer rate is due to high electro-catalytic effect and larger surface area of Ch@Ag

NPs. The shift of reduction peak potential of AZT towards more negative value with increasing scan rate reveals the irreversibility of electrochemical reduction of azido group of AZT [Vacek *et al.*, 2004]. Thus, 50 mV/s scan rate is optimized for studying the electrochemical reduction process as the reduction peak appearance is well defined with low over potential of AZT.

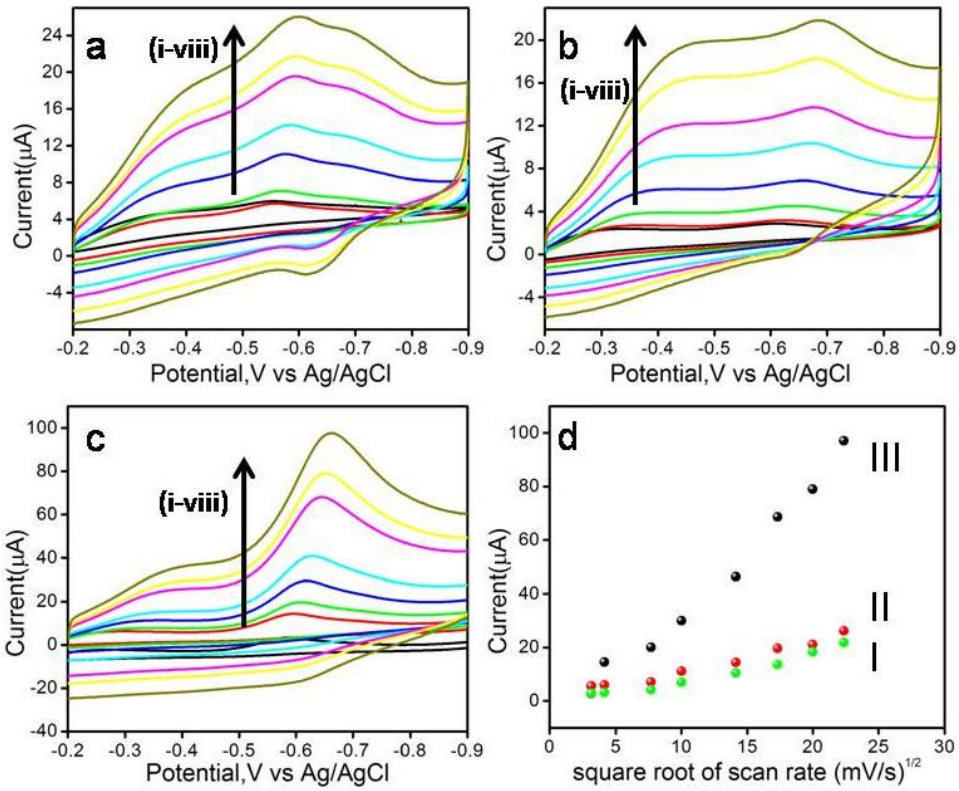

Figure 2.12 CV of (a) commercial GCE, (b) commercial Ag electrode, (c) Ch@Ag NPs/GCE at different scan rates from (i) 10, (ii) 20, (iii) 50, (iv) 100, (v) 200, (vi) 300, (vii) 400 and (viii) 500 mV/s in 0.1 M PBS (pH 7.6) and (d) plot of reduction current *vs.* square root of scan rate of (I) commercial Ag, (II) commercial GC electrode and (III) Ch@Ag NPs/GCE.

On the basis of above speculation, the electrochemical detection of AZT is carried out at various concentrations (above than 10 μM concentration which is toxic for human

beings) over Ch@Ag NPs/GCE and Ch@Ag NPs/SPGE at pH = 7.6 one by one as explained below.

2.3.3.2 AZT detection in PBS using Ch@Ag NPs/GCE

Ch@Ag NPs/GCE does not exhibit any well defined voltammetric signal in absence of AZT (in blank) in the potential window from -0.2 V to -1.0 V. This window is selected because the electro-reduction of AZT is expected in this range only. When a known amount of AZT is added in the supporting electrolyte (PBS, pH = 7.6), a well defined CV response is observed at -0.60 V *vs.* Ag/AgCl due to reduction of AZT. This suggests that the Ch@Ag NPs efficiently catalyses the reduction of AZT over the modified electrode surface. On serial addition of AZT in the concentration range of 74 µM to 718 µM, Ch@Ag NPs/GCE shows a substantial increase in reduction peak current owing to the excellent electro-catalytic effect of Ch@Ag NPs (as shown in Figure 2.13I). Herein Ch@Ag NPs/GCE, Ag NPs facilitates fast electron transfer kinetics due to its high electro-conductivity and larger surface area to volume ratio. After ninth serial addition of AZT in supporting electrolyte, we observe a decrease in the reduction peak current which represents the saturation of the electrochemical detection of AZT (as shown in calibration curve, Figure 2.13II) [Firrer *et al.*, 1973].The LOD and sensitivity of as-prepared Ch@Ag NPs/GCE is calculated by CV as 1 µM and 0.01 µA/µM respectively in PBS at S/N (Signal to noise ratio):3. In order to confirm the consistency in this CV results and also quantify the AZT detection at lower concentration level, differential pulse voltammetry (DPV) technique is applied using similar conditions as used for CV (as shown Figure 2.14). Herein this technique is used to get a Faradic response especially at the faster scan rates [Christie *et al.*, 1965; Zipper *et al.*, 1973; Firrer *et al.*, 1973]. We observed consistent results as in CV. Similar to CV results, we again

observed successive increase in reduction peak current on serial addition of AZT in PBS (pH = 7.6). But the stage of saturation of Ch@Ag NPs/GCE is observed herein after eleventh addition of AZT. This observation can be better visualized in corresponding calibration plot of DPV response as shown in Figure 2.14 (II). The LOD of as-prepared Ch@Ag NPs/GCE is calculated by DPV as 1 µM and sensitivity 0.022 µA/µM in PBS at S/N: 3.

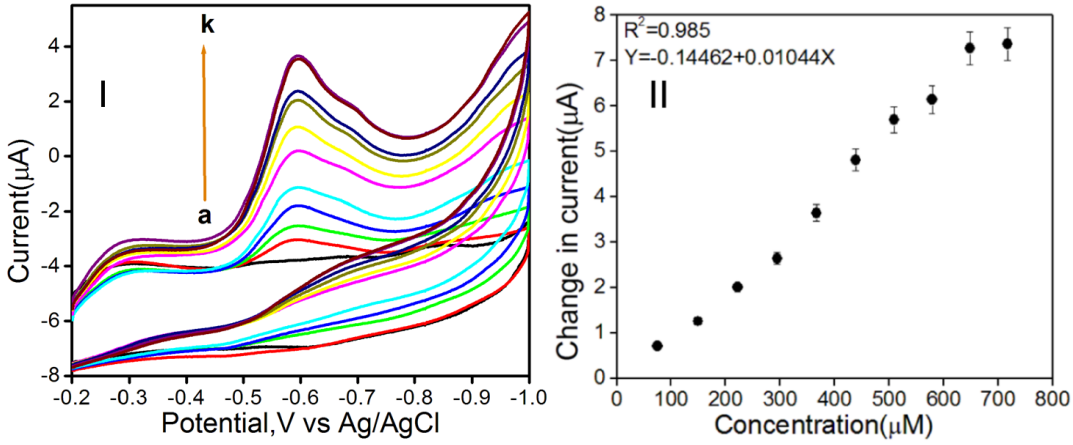

Figure 2.13 (I) CV response of Ch@Ag NPs/GCE in PBS at pH = 7.6 after serial addition of AZT from 74 µM to 718 µM concentration (a-k; a = blank current b = 75 µM, c = 149 µM, d = 222 µM, e = 295 µM, f = 367 µM, g = 439 µM, h= 509 µM, i = 579 µM, j = 649 µM, k = 718 µM) and (II) corresponding calibration plot showing AZT concentration *vs*. Change in reduction current with good correlation coefficient of 0.985.

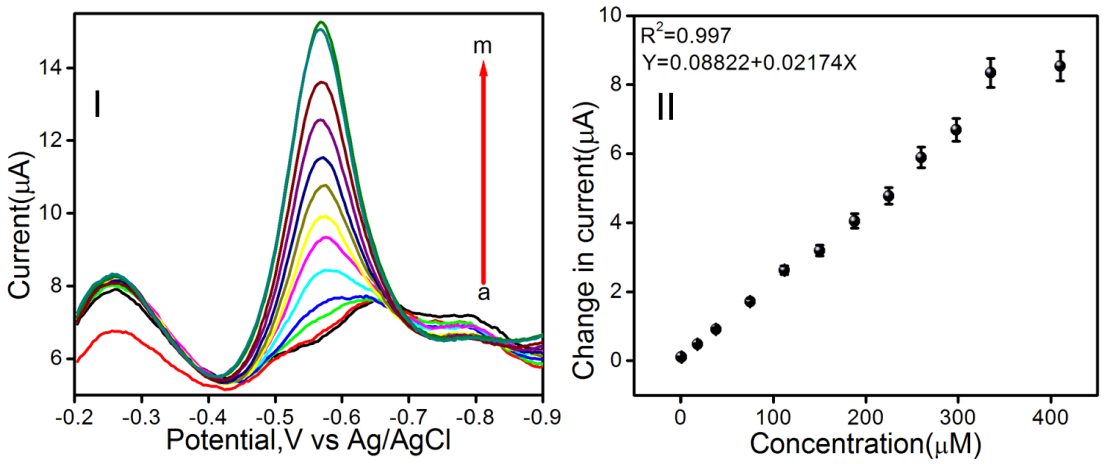

Figure 2.14 (I) DPV response of Ch@Ag NPs/GCE in PBS at pH = 7.6 after serial addition of AZT from 1 µM to 410 µM concentration (a-m; a = blank current, b = 1 µM, c = 8 µM, d = 38 µM, e = 75 µM, f = 112 µM, g = 150 µM, h = 188 µM, i = 225 µM, j = 260 µM, k = 298 µM, l = 335 µM, m = 410 µM) and (II) corresponding calibration plot showing AZT concentration *vs*. change in reduction current with good correlation coefficient of 0.997.

2.3.3.3 AZT detection in PBS and human plasma using Ch@Ag NPs/SPGE

After the successful determination of AZT on Ch@Ag NPs/GCE as explained earlier, Ch@Ag NPs material is further used for the modification of SPGE in order to make low cost and portable sensor for the detection of AZT in the concentration range of 10 µM to 533 µM in PBS (pH = 7.6) and human plasma (as shown in Figure 2.15). Fresh human plasma solution is used for experimentation purpose with the courtesy of our Institute Hospital. Prior to experimentation, it is diluted four times by deoxygenated high purity N_2 gas (99.99%) 0.1 M, pH = 7.6 PBS. We observe similar trend as seen earlier cases, on serial addition of AZT in PBS and in human plasma. The LOD and sensitivity of Ch@Ag NPs/SPGE is 1 µM and 0.015 µA/µM in PBS while it is 10 µM and 0.016 µA/µM in human plasma respectively at S/N: 3.This difference in LOD is

probably due to the presence of complex biological matrix in human plasma in comparison to PBS.

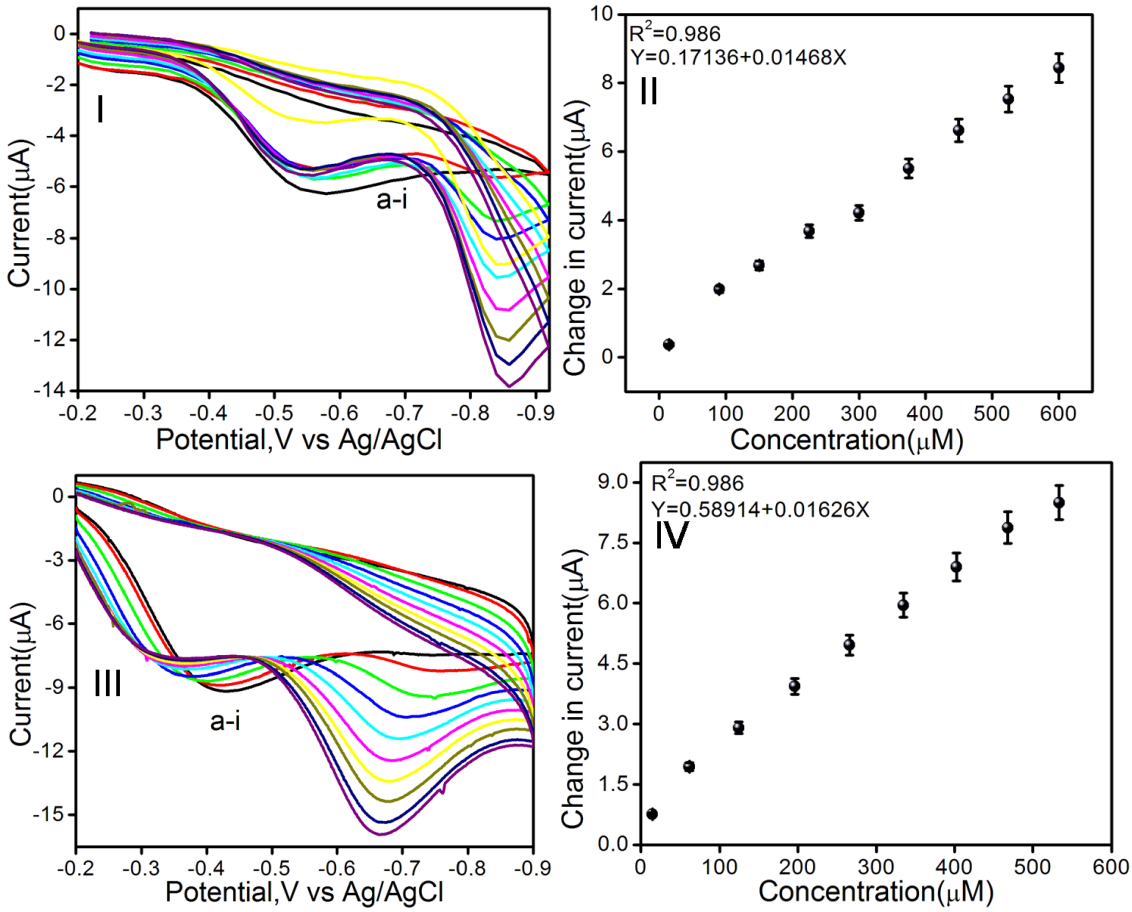

Figure 2.15 (I) CV response on Ch@Ag NPs/SPGE after serial addition of AZT from 10 µM to 600 µM concentration range (a-i; a = 10 µM, b = 90 µM, c = 150 µM, d = 225 µM, e = 300 µM, f = 375 µM, g = 450 µM, h = 525 µM, i = 600 µM) in PBS at pH = 7.6 with their corresponding calibration plot (II) with good correlation coefficient of 0.986 and (III) CV response on Ch@Ag NPs/SPGCE after serial addition of AZT from 10 µM to 533 µM concentration range (a-i; a = 10 µM, b = 62 µM, c = 125 µM, d =195 µM, e = 266 µM, f = 335 µM, g = 403 µM, h = 468 µM, i = 533 µM) in human plasma at pH = 7.6 with their corresponding calibration plot (IV) with good correlation coefficient of 0.986 (black line represents the blank current).

It is well known that nano particles have ability to agglomerate together due to its high surface energy. However, stabilization of such particles using polymers is one of the choices with slight compensation in its surface energy recognised for its activity. In case of Ch@Ag NPs, the role of Ch is to stabilize Ag NPs and provides availability for the interaction with electron rich species like AZT. During AZT detection over Ch@Ag NPs/SPGE in presence of phosphate buffer (pH=7.6), it is expected that AZT adsorbs on Ag surface (as shown in Figure 2.16) and azide group present in AZT exhibits electro-reduction to primary amine ($-NH_2$) on application of -0.60 V. After that this amino group undergoes protonation with available H^+ ions and leaving the surface of Ag NPs. Here this modification is showing large current and better detection limit in comparison to bare or without modified electrodes. This catalytic effect is explained based on coordination of AZT with modified electrode and large energetic surface of Ag NPs.

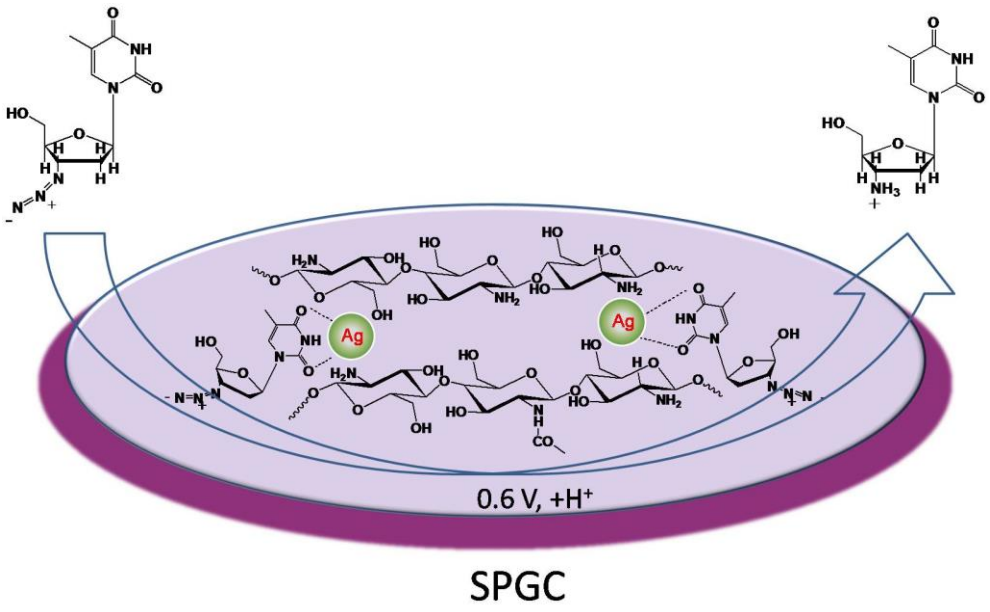

Figure 2.16 Proposed mechanism of AZT electro-catalysis over Ch@Ag NPs.

Simple CV technique is used to lower the cost of portable device and detection of AZT was demonstrated using low cost disposable SPGE up to the toxic level of the AZT, i.e., 10 µM. Further, we observe that the Ch@Ag NPs/SPGE does not suffer from electrode poisoning during AZT detection. Our sensing probe showed potential utility of sensor under real conditions. This sensor exhibits high stability and can be successfully utilised for the fabrication of AZT sensing devices.

Our as-fabricated sensing probe is disposable and cost effective. It has better capability to sense AZT in toxic dose range in human plasma and buffer solution compared to earlier reported works. A comparative study is summarized in Table 2.1 in this context.

2.4. Conclusion

Ch@Ag NPs hybrid material is synthesized successfully using chemical reduction method involves reduction of Ag salt assisted by $NaBH_4$ in presence of Chitosan as a stabilising agent. This as-synthesized material is well characterized first by various techniques like UV-visible, Zeta potential measurements, FT-IR, SEM, TEM, and EDAX for its structural and morphological properties. We observe that Ch@Ag NPs hybrid material consists of crystalline Ag NPs in Ch matrix which exhibits high dispersion stability in water. Thereafter, it is used as an active layer for the fabrication of sensing probes based on commercial GCE and SPGE and applied for AZT detection in toxic dose range (above 10 µM concentration). Electro-reduction of AZT is observed for sensing and detection using voltammetric technique. We observe that the reduction of AZT on modified electrode follows diffusion controlled process. The sensitivity of all electrodes is almost same with different LODs. The LOD of Ch@Ag NPs/GCE and Ch@Ag NPs/SPGE is observed as 1 µM in PBS. Similarly, the LOD of Ch@Ag NPs/SPGE is 10 µM in human plasma. Our proposed portable sensor (Ch@Ag

NPs/SPGE) is highly reliable for clinical application and laboratory detection of AZT.

Table 2.1 Comparative study for previously reported AZT detections by electrochemical methods.

S. No.	**Modified electrode/Ref.**	**Supporting electrolyte**	**Reduction potential, V *vs.* Ag/AgCl**	**Linear response range**	**AZT detection in real sample**	**Portable sensor probe**
1	HMDE [Vaeck *et al.*, 2004]	PBS 0.1 M; pH = 8	-1.1	500 pM-1.0 µM	-	-
2	HMDE [Leandro *et al.*, 2010]	PBS 0.1 M; pH = 8	-0.96	0.4-1500 µM	-	-
3	Ag solid amalgam electrode [Peckova *et al.*, 2009]	Borate buffer 0.05 M; pH = 9.3	-1.05	0.25 - 1.25 µM	-	-
4	Graphite paste electrode [Mohan *et al.*, 2010]	1 mM tris-HCl; pH = 6	0.08	1 -100 µM	-	-
5	Ag-NF/M-MWCNT/GCE [Rafati *et al.*, 2014]	PBS 0.1 M; pH = 7	-0.66		Human plasma	-
6	Ch@Ag NPs/GCE and Ch@Ag NPs/SPGE	PBS 0.1 M; pH = 7.6	-0.60	1 -718 µM	Human plasma	Present Work

.